

## QCD ISSUES AT THE TEVATRON

BRENNA FLAUGHER

*M.S. 318 P.O. Box 500 Fermilab, Batavia, IL 60510 USA*

*E-mail: brenna@fnal.gov*

The status of QCD studies at the Fermilab Tevatron are discussed. Specifically, the measurements of inclusive jet cross sections from the CDF and D0 collaborations are compared to theoretical predictions. New measurements in the forward rapidity regions are described and multijet results are discussed.

### 1 Introduction

The Fermilab  $p\bar{p}$  collider, with a center of mass energy of 1.8 TeV, provides unique opportunities to study QCD at the highest  $E_T$ . The Run 1 data samples from CDF and D0, roughly  $100 \text{ pb}^{-1}$  per experiment, allow precision tests of QCD predictions. Comparisons between data and theory are discussed below for jet identification, inclusive jet and dijet cross sections as well as multijet event distributions.

### 2 Jet Identification

The identification of jets is fundamental to the comparison between data and theoretical predictions. Ideally, measurements and theory would use identical algorithms. In practice this is not precisely possible because the predictions are based on parton level calculations with 2 or 3 partons in the final state<sup>1,2</sup>, while the experiments measure clusters of hadrons<sup>3</sup>. The Snowmass cone algorithm<sup>4</sup> was defined with the goal of establishing a standard algorithm for use in both experiment and theory. Partons, or hadrons, which fall within a cone of radius  $R$  ( $R = \sqrt{\delta\eta^2 + \delta\phi^2} = 0.7$ ) are merged into one “jet”. Both CDF and D0 use a modified Snowmass cone algorithm to identify the jets in the detectors<sup>3</sup>. The primary difference with the theory comes from the treatment of close or overlapping jets. In the data, jets are combined if they overlap significantly (share a fraction of  $E_T$ ) and otherwise they are separated. Studies found the introduction of an additional parameter to the theory,  $R_{sep}$ , allows the parton level predictions to more closely mimic the algorithm used on the data<sup>5</sup>. Partons are merged into one jet if they are within  $R_{sep} * R$ , where  $R_{sep} = 1.3$ .

### 3 Inclusive Jet Cross Section

Measurement of the inclusive jet cross section provides a powerful test of QCD over a wide range of jet  $E_T$  ( $\approx 40\text{-}500 \text{ GeV}$ ) while the cross section falls by roughly 8 orders of magnitude. It provides information about the parton

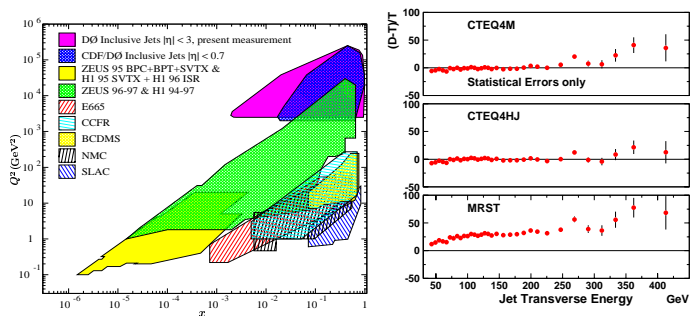


Figure 1. Left: Ranges of  $x$  and  $Q^2$  covered by different jet measurements. Right: CDF Run 1B data compared to predictions with 3 PDFs (EKS,  $\mu=E_T/2$ ,  $R_{sep}=1.3$ ) for  $:0.1 \leq |\eta| \leq 0.7$ .

Table 1.  $\chi^2$  and relative probability for different predictions

PDF	$\chi^2$	$CL(\%)$	$\chi^2 - \chi_{cteq4hj}^2$	P Rel. to CTEQ4HJ
CTEQ4HJ	46.8	10	0.0	1
MRST	49.6	7.4	2.7	0.5
CTEQ4M	63.4	1.4	16.6	$10^{-3}$

distribution functions (PDFs) and the strong coupling constant over a large kinematic region. At the highest  $E_T$ , it probes the structure of the proton to a scale of  $\approx 10^{-17}$ cm. Figure 1(left) shows the kinematic regions covered by the inclusive jet measurements and by other experiments.

In 1996 CDF published a result<sup>6</sup> from the Run 1A data sample( $19\text{pb}^{-1}$ ) which indicated an excess of jets were produced relative to the theoretical predictions at high  $E_T$  for jets with  $0.1 \leq |\eta| \leq 0.7$ . This motivated an intense reevaluation of the uncertainty in the theory, and the derivation of a new PDF (CTEQ4HJ)<sup>7</sup>. With a new and more flexible parameterization of the gluon distribution, it was possible to obtain much better agreement with the CDF data. CDF recently published the results from the run 1B data sample ( $87\text{pb}^{-1}$ ), shown in Fig. 1(right), which is good agreement with the Run 1A measurement<sup>8</sup>. The analysis of the Run 1B data uses a relative  $\chi^2$  technique to compare the different predictions<sup>8</sup>. These results are shown in Table 1. The CTEQ4HJ prediction is favored over MRST by a factor of 2 and over most of the other predictions by a factor of more than 100.

D0 has published measurements of the central inclusive jet cross section in two rapidity regions<sup>9</sup>. Figure 2 shows the D0 data compared to predictions in the  $0.1 \leq |\eta| \leq 0.7$  region (left) and a comparison to the CDF result (right). Good agreement is observed between the D0 data and theory with all the PDFs. There is also good agreement between the two experiments.

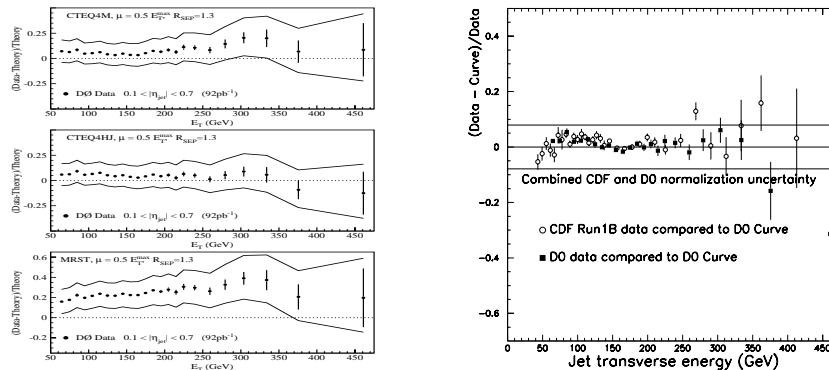


Figure 2. Left: D0 Run 1B data ( $0.1 \leq |\eta| \leq 0.7$ ) compared to predictions. Right: Comparison of the CDF and D0 data to a smooth curve describing the D0 data. The 2.7% difference in relative normalization has been corrected.

Table 2. Results from comparison of the D0 data to theoretical predictions for the inclusive jet cross section at  $\sqrt{s} = 0.630$  TeV, the ratio of the cross sections at 0.630 and 1.8 TeV and the average ratio over the  $E_T$  range of the measurement.

PDF	$\frac{d\sigma}{dE_T}$ $\chi^2$ for 20 DOF	Ratio $\chi^2$ for 20 DOF	Avg. Ratio $\chi^2$ for 1 DOF
CTEQ4M	24.1	22.4	10.7
CTEQ4HJ	18.8	21.0	13.2
MRST	22.6	22.2	12.6

#### 4 Test QCD scaling

In Run 1B, CDF and D0 measured the inclusive jet cross sections at  $\sqrt{s}=1.8$  and 0.630 TeV. Scaling predicts that dimensionless quantities are independent of  $\sqrt{s}$  while QCD predicts scaling violations due to the running of  $\alpha_s(\mu)$  and the evolution of the PDFs. Previous CDF results<sup>10</sup> could rule out scaling, but the agreement with QCD predictions was poor, particularly at low  $E_T$ . Figure 3(left) shows the comparison of the CDF and D0 results<sup>11,12</sup> to theory. The CDF data is in good agreement with previous results. Good agreement between CDF and D0 data sets is observed at high  $E_T$ , but the measurements diverge at low  $E_T$ . This is potentially due to different treatment of the underlying event energy by the two experiments. Figure 3(right) shows the D0 results for the inclusive cross section at  $\sqrt{s}=0.630$  TeV and Table 2 shows the results of fits to the data. The normalization of the predictions for the ratio is systematically above the data, independent of the choice of PDF.

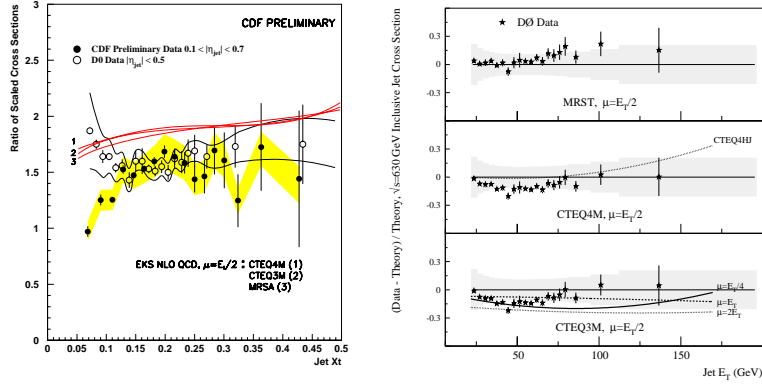


Figure 3. Left: The ratio of cross section at 0.630 and 1.8 TeV from CDF and D0. Right: The D0 inclusive jet cross section at  $\sqrt{s}=0.63$  TeV compared to predictions.

## 5 Rapidity Dependence of Jet Cross Sections

The rapidity dependence of the inclusive and dijet cross sections provides information about new regions of  $x$  and  $Q^2$ . Figure 1(left) shows the new low  $x$  region covered by the inclusive cross section measurements at high rapidity. Figure 4(left) shows the comparison of the D0 data<sup>13</sup> in the different rapidity bins to the theoretical predictions with CTEQ4HJ. CDF measured the di-jet differential cross section, where one jet is constrained to the central ( $0.1 \leq |\eta| \leq 0.7$ ) region and the other jet is restricted to different rapidity regions<sup>14</sup>. This measurement probes regions of both low and high  $x$ . Figure 4(right) shows the CDF data compared to the theoretical predictions.

## 6 Ratio of 3-jet to 2-jet Cross Sections

The ratio of 3-jet to 2-jet cross sections indicates the rate of gluon emission in jet production, minimizes the sensitivity to systematic uncertainties in the cross section and is insensitive to the choice of PDF. Figure 5(left) shows the ratio for three different 3<sup>rd</sup> jet thresholds, plotted as a function of  $H_T$ , where  $H_T$  is the sum  $E_T$  of the jets in the event. The predictions for this ratio are sensitive to the choice of renormalization scale. Figure 5(right) shows the comparison to the data with a 20 GeV jet threshold for various scales. In particular, the analysis compared one scale per event to having a separate scale ( $\mu^{(3)}$ ) for the third jet. When all three jet  $E_T$  thresholds are considered, one scale per event, equal to  $0.3H_T$ , provides the best fit to the data.

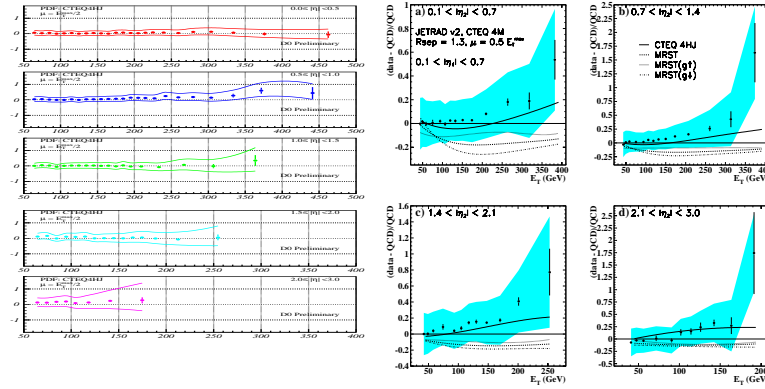


Figure 4. Left: Percent difference between D0 inclusive jet cross section data and theoretical predictions with CTEQ4HJ PDFs in different rapidity bins. Right: Percent difference between CDF dijet differential cross section and theoretical predictions with four PDFs.

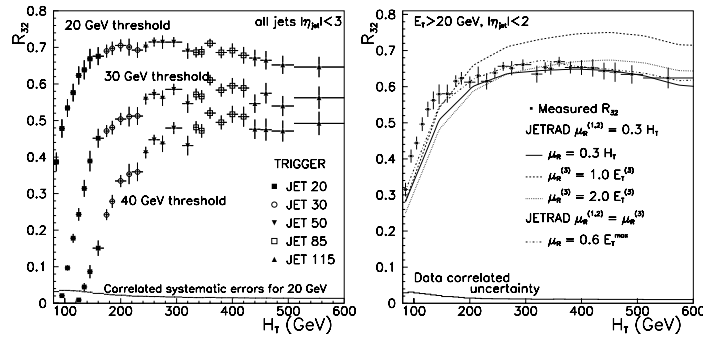


Figure 5. Left: The ratio of 3-jet to 2-jet cross sections as a function of the sum  $E_T$  of the jets for different jet thresholds. Right: Comparison of data (with a 20 GeV cut on the  $3^{rd}$  jet) and theoretical predictions with different choices of renormalization scale (D0).

## 7 Multijet events

CDF and D0 have both carried out studies of multijet events<sup>16,17</sup>. Detailed comparison to predictions have found that while both HERWIG<sup>18</sup> and NJETS<sup>19</sup> do a reasonable job describing data with up to 6 jets, the NJETS program is closer to the data than HERWIG at the edges of phase space.

## 8 Conclusions and Prospects

The central inclusive jet cross sections are consistent with QCD predictions over 8 orders of magnitude given the current flexibility in the theory due to the PDFs. New results on rapidity dependence of the cross sections can provide

better constraints on the PDFs. The ratio of the cross sections at  $\sqrt{s}=0.630$  and 1.8 TeV shows that the predictions are systematically higher than the measurements, independent of PDFs. The ratio of 3-jet to 2-jet production provides information about the best choice of renormalization scale for future studies. We are eagerly looking forward to Run 2. With improved detectors, a higher center of mass energy (1.96 TeV) and a data sample of  $2 \text{ fb}^{-1}$ , we will have  $\approx 40$  times the data above 400 GeV or roughly 1000 very high  $E_T$  jet events per experiment.

## References

1. S. Ellis, Z. Kunszt, and D. Soper, Phys. Rev. Lett. **62** 2188 (1989); Phys. Rev. Lett. **64** 2121 (1990); Phys. Rev. D **40** 2188 (1989).
2. W. T. Giele, E.W.N. Glover and D.A. Kosower, Nucl. Phys. **B403** 633 (1993).
3. G. Blazey and B. Flaughner, Annu. Rev. Nucl. Part. Sci. **Vol. 69** 633 (1999).
4. J. Huth *et al.* "Proceedings 1990 Summer Study on High Energy Physics, ed. E Berger. Singapore: World Scientific, 134 (1992).
5. S.K. Ellis, Z. Kunszt, D. Soper, Phys. Rev. Lett. **69** 3615 (1992) and S. Ellis CERN-TH-6861-93 In proceedings of 28th Rencontres de Moriond: QCD and High Energy Hadronic Interactions, Les Arcs, France, 20-27 Mar 1993. hep-ph/9306280.
6. F. Abe *et al.* (CDF Collaboration), Phys. Rev. Lett. **77** 438(1996).
7. J. Huston *et al.*, Phys. Rev. Lett. **77**, 444(1996).
8. F. Abe *et al.* (CDF Collaboration), FERMILAB-PUB-01/008-E, submitted to PRD.
9. B. Abbot *et al.* (D0 Collaboration), Phys.Rev.Lett. **82**, 2451 (1999).
10. F. Abe *et al.* (CDF Collaboration), Phys. Rev. Lett. **70** 1376 (1993) .
11. A. Akopian, Ph.D. Thesis (CDF Collaboration), Rockefeller University UMI-99-27900-mc (1999).
12. B. Abbott *et al.* (D0 Collaboration) FERMILAB-PUB-00-216-E, Submitted to Phys.Rev.D; hep-ex/0012046. FERMILAB-PUB-00-213-E, Submitted to Phys.Rev.Lett. hep-ex/0008072.
13. B. Abbott *et al.* (D0 Collaboration) Phys.Rev.Lett. **86**1707 (2001).
14. F. Abe *et al.* (CDF Collaboration), FERMILAB-PUB-00/311-E, submitted to Phys. Rev. D.
15. B. Abbott *et al.* (D0 Collaboration) Phys.Rev.Lett.**86** 1955 (2001).
16. F. Abe *et al.* (CDF Collaboration), Phys.Rev. **D56** 2532 (1997); Phys.Rev. **D54** 4221 (1996); Phys.Rev.Lett.**75** 608 (1995); Phys.Rev. **45** 2249 (1992).
17. B. Abbott *et al.* (D0 Collaboration) Phys. Lett. **B414** 419 (1997).
18. G. Marchesini and B. R. Webber, Nucl. Phys. **B310**, 461 (1988).
19. F.A. Berends, W. Giele, and H. Kuijf, Nucl. Phys. **B333**, 120(1990).